3-2002

L-Arginine Uptake and Metabolism Following in vivo Silica Exposure in Rat Lungs

Leif D. Nelin
University of New Mexico

Gary S. Krenz
Marquette University, gary.krenz@marquette.edu

Louis G. Chicoine

Christopher A. Dawson
Medical College of Wisconsin

Ralph M. Schapira

American Journal of Respiratory Cell and Molecular Biology, Vol. 26, No. 3 (2002): 348-355. DOI.

L-Arginine Uptake and Metabolism following *in vivo* Silica Exposure in Rat Lungs

Leif D. Nelin
Ohio State University
Gary S. Krenz
Marquette University
Louis G. Chicoine
Nationwide Children's Hospital
Christopher A. Dawson
Tidewater Physicians
Ralph M. Schapira
Clement J. Zablocki Veterans Affairs Medical Center

Abstract

Pulmonary inflammation increases nitric oxide (NO) production via inducible nitric oxide synthase (iNOS). This study was performed to determine some of the factors that affect the availability of the NOS substrate, l-arginine (l-arg), in the intact lung subjected to silica-induced inflammation. Nitrate production, as an index of NO production, was significantly greater in silica-exposed lungs (53.5 ± 12.1

nmol/90 min) compared with controls (22.5 ± 5.1 nmol/90 min, $P < 0.05$). This was accompanied by greater ($P < 0.0001$) 90-min [^{3}H]l-arg uptake (62 ± 3% control, 82 ± 1% silica), a significantly ($P < 0.005$) increased permeability-surface area product for l-arg (0.28 ± 0.05 ml/min control, 0.63 ± 0.07 ml/min silica), and a significantly ($P < 0.001$) increased urea production (1.16 ± 0.08 μ mol/90 min control, 1.77 ± 0.06 μ mol/90 min silica). There was no difference in eNOS protein between groups and eNOS mRNA was not detectable in either group, whereas silica exposure resulted in the appearance of both iNOS protein and mRNA. Silica exposure increased CAT-1 and CAT-2 mRNA ~ 8-fold compared with controls. We conclude that the increase in NO production in silica-exposed lungs was associated with increased l-arg uptake from the vasculature, presumably resulting from increased CAT-1 and CAT-2, and by increased l-arg metabolism via arginase.

Pulmonary inflammation such as occurs with silica exposure in rats involves recruitment and activation of alveolar macrophages and neutrophils[1, 2]. The macrophages and neutrophils isolated from the bronchoalveolar lavage of lungs from silica-exposed rats have increased nitric oxide (NO) production[3, 4], and the increased NO production plays an important role in the silica-induced inflammatory process. Nitric oxide synthase (NOS) metabolizes l-arginine (l-arg) to NO and l-citrulline. The enzyme arginase (AR) also metabolizes l-arg to form urea and l-ornithine (l-orn). l-orn can then be metabolized to form polyamines and proline, which are important in wound healing, angiogenesis and cardiovascular function[5]. Studies in aortic endothelial cells suggest that AR may have a regulatory role in polyamine and proline synthesis[6]. Thus, the regulation of NOS and AR activities in inflammatory lung disease may determine the balance between inflammatory lung injury due to NO production and lung repair due to polyamine and proline synthesis. In cell studies, it has been found that AR activity is upregulated in various models of inflammatory lung injury[7-9]. Furthermore, in rat lung, treatment with LPS induced the expression of both iNOS and arginase[10]. Because inflammation increases lung metabolism of l-arg by both NOS and AR, this increase in l-arg metabolism may deplete lung l-arg unless l-arg uptake is also increased by inflammation. In cultured pulmonary arterial endothelial cells and pulmonary vascular smooth muscle cells, treatment with cytokines induced iNOS and increased l-arg uptake[11-14]. These studies raise the possibility that l-arg uptake and/or alternative metabolic pathways for l-arg may be targets for therapeutic manipulation of NO production in inflammatory diseases such as those caused by silica exposure. Therefore, we addressed the question of whether in a condition such as silica exposure, wherein iNOS activity is elevated in the intact lung, l-arg uptake from the vasculature and/or l-arg metabolism via arginase would also be affected.

We studied isolated perfused lungs from either control rats or rats exposed to 50 mg silica 3–14 d before study. We measured the uptake of [^{3}H]l-arg from the perfusate into the lung, and the accumulation of nitrite/nitrate (NO_X) and urea in the lung perfusate. To differentiate between actual increases in l-arg uptake versus changes in lung cell composition caused by silica exposure, we developed a mathematical model to describe the changes in l-arg uptake seen with silica exposure. Finally, to correlate the mathematical model interpretation with the molecular events involved in increased l-arg metabolism and uptake, lungs were harvested for measurement of eNOS and iNOS mRNA and protein, and for cationic amino acid transporter-1 (CAT-1) and CAT-2 mRNA.

Materials and Methods

Silica Exposure

Silica-induced inflammatory lung injury was produced as previously described[7, 15, 16]. Sprague-Dawley rats (250–300 g) were anesthetized with 30 mg/kg sodium pentobarbital intraperitoneally. The trachea was intubated with polyethylene tubing (PE-240; Becton Dickinson, Sparks, MD) via the mouth. Then 50 mg of SiO_2 (Pennsylvania Glass and Sand, Pittsburgh, PA) in 0.3 ml sterile 0.9% saline was instilled into the trachea via the PE-240 tubing. Following instillation the rats were allowed to recover from the anesthetic, and then returned to the animal facility where they remained for 3–14 d with *ad libitum* access to food and water.

Isolated Lungs

An isolated rat lung preparation was used as previously described[15, 16]. The rat was anesthetized with sodium pentobarbital (50 mg/kg) intraperitoneally. A catheter was placed in a carotid artery. Heparin (1,250 U/kg) was given intra-arterially and the animal exsanguinated via the carotid artery catheter. The main pulmonary artery, the left atrium, and the trachea were cannulated and the lungs were placed in a perfusion chamber. The perfusion system was a recirculating system maintained at 37°C. The perfusate was a Krebs–Ringer bicarbonate buffer solution containing 5% dextran (KRB). The perfusate was pumped (Masterflex roller pump, Cole-Parmer, Bannington, IL) into the pulmonary artery at 15 ml/min from a reservoir into which perfusate drained from the left atrium. The pulmonary arterial pressure (Pa) was recorded continuously throughout the perfusion period. The lungs were ventilated using a piston-type ventilator (Harvard Apparatus, Dover, MA) with a tidal volume of 5 ml, using a gas mixture containing 15% O_2, 6% CO_2, and balance N_2. The dynamic compliance (Cdyn) was calculated as the tidal volume divided by airway pressure excursion. At the end of the perfusion period the lungs were weighed and then placed in a drying oven until a constant dry weight was obtained.

l-Arginine Uptake

The perfusion circuit contained two reservoirs in parallel, such that the perfusate entering the lung could be rapidly changed from one reservoir system to the other. Initially, both reservoirs contained the KRB, but only one reservoir was included in the recirculating system. l-[2,3,4,5-^{3}H] arginine monohydrochloride (7.5 µCi, specific activity 59 Ci/mmol; Amersham Life Science, Arlington Heights, IL) was added to the KRB in the other reservoir during the 10–15 min stabilization period to allow for adequate mixing in the perfusate, the final concentration of [^{3}H]l-arg was ~ 10 nM. In some experiments unlabeled l-arg was also added to the perfusate along with the [^{3}H]l-arg as indicated below. Once the preparation had stabilized, a zero time sample was taken from the reservoir containing the [^{3}H]l-arg. Then the perfusate entering the lung was rapidly switched to the [^{3}H]l-arg reservoir. The perfusate leaving the lungs was discarded until the volume of perfusate in the lung and the tubing from the lung to the reservoir at the time of the switch were filled with the KRB containing the [^{3}H]l-arg. Then recirculating perfusion from the [^{3}H]l-arg reservoir was established. The perfusate in the reservoir was sampled at 5, 10, 15, 30, 45, 60, 75, and 90 min after switching to the [^{3}H]l-arg reservoir. Each sample (200 µl) was placed in 5 ml liquid scintillation counting cocktail (Bio-Safe II; RPI, Mount Prospect, IL) and counted. The ^{3}H uptake was then determined from the amount of ^{3}H added, the perfusate volume, and the ^{3}H in the perfusate at each sample time. The amount of [^{3}H]l-arg taken

up was determined from the ratio of ^{3}H in l-arg to that in its ^{3}H metabolites for each sample time as described under thin-layer chromatography.

To determine if *in vivo* silica exposure had an effect on the uptake and metabolism of l-arg by the lung, [^{3}H]l-arg uptake was measured as described above in five lungs from control rats and eight lungs from rats instilled with silica. At the end of the 90-min perfusion period, perfusate was sampled for determination of NO_X and urea.

To determine the specificity of the l-arg uptake, [^{3}H]l-arg uptake was measured as described above in an additional six lungs from control rats and six lungs from rats instilled with silica. In these isolated lungs a saturating concentration of unlabeled l-arg was included in the perfusate. For the lungs from control rats 20 mM ($n = 3$), 60 mM ($n = 2$), or 150 mM (n = 1) unlabeled l-arg was included in the perfusate. For the lungs from silica instilled rats 40 mM ($n = 2$), 100 mM ($n = 2$), or 150 mM ($n = 2$) unlabeled l-arg was included in the perfusate.

l-Glucose Uptake

To estimate the extracellular tissue volume and the permeability surface area product (*PS*) for its accessibility to [^{3}H]l-glucose, the uptake of [^{3}H]l-glucose was measured in five lungs from control rats and five lungs from rats instilled with silica. l-Glucose (l-glc) is a hydrophilic molecule of about the same size as l-arg but confined to the extracellular volume. The same procedure was used as described above except that l-1-[^{3}H(N)]glucose (15 µCi, specific activity 20 Ci/mmol; DuPont NEN, Boston, MA) instead of [^{3}H]l-arg was added to the KRB in the second reservoir.

Thin-Layer Chromatography

The fraction of ^{3}H in [^{3}H]l-arg was determined using thin-layer chromatography (TLC). A sample of the perfusate (40 µl) was streaked directly on a TLC plate (Silica Gel 60 F_{254}; EM Science, Darmstadt, Germany), which was run in a mobile phase consisting of chloroform/methanol/ammonium hydroxide/water (9:9:4:1). The TLC plate was scraped in 1-cm bands into a scintillation vial, 10 ml of scintillation fluid was added, and the vial was placed in a sonicator for 30 s and then into a liquid scintillation counter. The R_f values are 0.18 for l-arg, 0.31 for l-ornithine, 0.66 for l-citrulline, and 1.00 for l-argininosuccinate in this system.

Nitrite/Nitrate Assay

Perfusate samples were assayed in duplicate for nitrite/nitrate (NO_X) using a chemiluminescence nitric oxide analyzer (Sievers, Boulder, CO). A quantity of 100 µl of sample was injected into a reaction chamber containing a mixture of vanadium (III) chloride in 2 M HCl heated to 90°C to reduce NO_X to NO gas. The NO gas was carried into the analyzer using a constant flow of N_2 gas. The analyzer was calibrated using a $NaNO_3$ standard curve.

Urea Assay

Perfusate samples were assayed in triplicate for urea colorimetrically as previously described[7, 17]. A quantity of 100 µl of sample was added to 3 ml of chromogenic reagent (5 mg thiosemicarbazide, 250 mg diacetyl monoxime, 37.5 mg $FeCl_3$ in 150 ml 25% [vol/vol] H_2SO_4), or the same reagents plus 0.5 units urease. After 1 h at 37°C, the mixtures were vortexed and then boiled at 100°C for 5 min. The

mixture was cooled to room temperature and the difference in absorbance (530 nm) with and without urease was determined and compared with a standard curve prepared with urea.

Western Blots

The lungs were assayed for NOS protein using Western blot analysis as previously described[18]. The lungs were harvested, immediately placed in liquid N_2, and stored at −70°C until the day of assay. Lung tissue was thawed and then homogenized in 25 mM Tris HCl buffer containing 1 mM EDTA, pH 7.4, using a Polytron blender. Aliquots of the homogenate were diluted 1:1 with sodium dodecyl sulfate sample buffer, heated to 80°C for 15 min, and then centrifuged at 10,000 × *g* at room temperature for 2 min. Aliquots of the supernatant were used for sodium dodecyl sulfate-polyacrylamide gel electrophoresis. The proteins were transferred to nitrocellulose membranes, and the membranes blocked overnight in phosphate-buffered saline with 0.1% Tween containing 10% nonfat dried milk. The membranes were incubated with the primary antibody, eNOS (Transduction Laboratories), or iNOS (Transduction Laboratories) 1:500 for 1 h and then washed with PBS-T with 1% nonfat dried milk. The membranes were incubated with the biotinylated IgG secondary antibody (Vector Laboratories) 1:5,000 for 30 min, washed, and then incubated with streptavidan-horseradish peroxidase conjugate (1:1,500) for 30 min. The bands for eNOS and/or iNOS were visualized using chemiluminescence and quantified using densitometry (Scion Image; Scion Corp, Frederick, MD). Authentic eNOS and iNOS (Transduction Laboratories) were used as positive controls.

Reverse Transcription/Polymerase Chain Reaction Assay

Lungs were harvested, immediately placed in liquid nitrogen, and stored at −70°C until the day of assay. Total cellular RNA isolated and purified from crushed frozen lungs by the acid phenol guanidinium method[19]. Reverse transcription (RT) reactions (40 µl) contained 1.0 µg of total cellular RNA, 18 U AMV reverse transcriptase (Promega), 2.5 µM oligo-d$(T)_{16}$ (Perkin-Elmer, Boston, MA), 1.0 mM dNTPs, and AMV-RT buffer (Promega). The reactions were incubated at room temperature for 10 min, 42°C for 1 h, and 94°C for 5 min. Polymerase chain reactions (PCRs) contained 1.0 µM specific oligonucleotide primers for either eNOS (forward 5′-TACGGAGCAGCAAATCCAC-3′, reverse 5′-CAGGCTGCAGTCCTTTGAT-3′), iNOS (forward 5′-GAC ATCGACCAGAAGCTGTC-3′, reverse 5′-GGGCTCTGTTGA GGTCTAAAG-3′), CAT-1 (forward 5′-GCCATCGTCATCTC CTTCCTG-3′, reverse 5′-CCCTCCCTCACCGTATTTCAC-3′), or CAT-2 (forward 5′-AACGTGCTTTTATGCCTTTGT-3′, reverse 5′-GGTGACCTGGGACTCGCTCTT-3′)[14, 20, 21]. Additional components of the PCR reaction included 5.0 µl of RT product, 3 mM $MgCl_2$, 1× PCR Buffer-D (Invitrogen), 1 mM dNTPs, and 1 U Amplitaq polymerase (Perkin-Elmer). PCR reactions were denatured at 94°C for 4 min and then cycled at 94°C for 1 min, 53°C for 1 min, and 72°C for 2 min, for a total of 30 cycles. Final extension was for 5 min at 72°C. PCR products were visualized and sized by 1.5% agarose gel-electrophoresis. Gels were photographed using Polaroid 667 film and digitized using an Epson 636 scanner. Band density analysis was performed using Scion Image (Scion Corp.). The PCR product sizes were the expected 819, 575, 531, and 613 bp for eNOS, iNOS, CAT-1, and CAT-2, respectively.

Data Analysis

To determine if any change in l-arg uptake was due to simply to changes in cellular composition of the lung, or whether a change in transporter activity was involved, a mathematical model to describe the

uptake of tracer quantities of l-arg was developed. The first step in the model was to fit a single exponential of the form

$$y = \mathrm{A}e^{-\alpha t} + k(1)$$

Equation 1

was fit to the [^{3}H]l-glc data. Because l-glc is a molecule of about the molecular weight of l-arg, and it is neither metabolized nor actively transported by the lung, l-glc was used as a marker of changes in the extravascular space accessible by diffusion. The resulting rate constant (α) was used to calculate the permeability-surface area product ($\mathrm{PS_{glc}}$) as previously described[22] from equation 2

$$\mathrm{PS_{glc}} = \alpha Q_1 \left(1 - \frac{\mathrm{Ceq}}{C_0}\right)$$

Equation 2

where Q_1 is the total system perfusate volume, *Ceq* is the equilibrium concentration of [^{3}H]l-glc, and C_0 is the concentration of [^{3}H]l-glc at time 0. The extracellular tissue volume (Q_2) into which the [^{3}H]l-glc could diffuse was calculated using the following equation

$$Q_2 = \frac{(C_0 Q_1 - \mathrm{CeqQ_1})}{(\mathrm{Ceq})}$$

Equation 3

The tracer concentration l-arg kinetics was modeled as first order with the flux of l-arg between compartments represented by permeability surface area products. Because the arterial venous difference during the experiments was found to be small, any axial capillary concentration gradients could be ignored and the l-arg uptake process modeled using ordinary differential equations. l-Arg mass balance results in the system:

$$Q_1 \frac{\mathrm{dc_1}}{\mathrm{dt}} = -(\mathrm{PS})_1(c_1 - c_3) - (\mathrm{PS})_2(\mathrm{c_1} - \mathrm{c_2})$$

Equation 4

$$Q_2 \frac{\mathrm{dc_2}}{\mathrm{dt}} = -(\mathrm{PS})_1(c_2 - c_3) + (\mathrm{PS})_2(\mathrm{c_1} - \mathrm{c_2})$$

Equation 5

$$Q_3 \frac{\mathrm{dc_3}}{\mathrm{dt}} = (\mathrm{PS})_1(c_1 - c_3) + (\mathrm{PS})_2(\mathrm{c_2} - \mathrm{c_3}) - \mathrm{kc_3}Q_3$$

Equation 6

where Q_1 denotes the known reservoir, lung, tubing system volume, minus previous samples drawn for measurement; Q_2 denotes the measured extracellular volume (obtained from the l-glc distribution) accessible to l-arg; Q_3 denotes a virtual intracellular volume, accounting for both an actual volume and potentially rapid binding and unbinding to nonspecific sites, l-arg is assumed to be metabolized in this

volume; *k* denotes the l-arg metabolism rate in Q_3; $(PS)_1$ is the permeability surface area product for bidirectional movement of l-arg between either Q_1 or Q_2, and Q_3; $(PS)_2$ is taken to be equal to the measured $\mathrm{PS_{glc}}$ permeability surface area product between Q_1 and Q_2; c_1 denotes the [^{3}H]l-arg concentration within Q_1; c_2 denotes the [^{3}H]l-arg concentration within Q_2; and c_3 denotes the [^{3}H]l-arg concentration within Q_3, the model is illustrated in Figure 1. The Q_2 compartment was included in the mathematical model to account for the potential for increased l-arg uptake due solely to dilutional effects. Because only tracer concentrations were used the underlying system of equations is linear, and the measured concentrations were normalized to the initial concentration such that c_1 was initially set to unity and c_2 and c_3 to 0 (Figure 2).

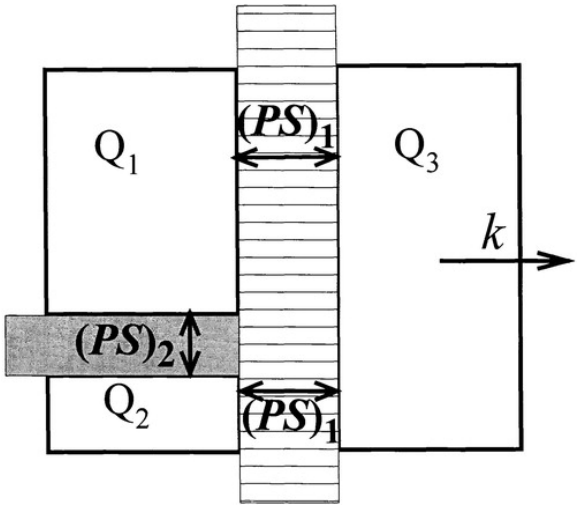

Fig. 1. Illustration of the mathematical model described in equations 4–6. Q_1 represents the vascular volume, Q_2 represents the extravascular volume, and Q_3 represents the intracellular volume. l-arg is assumed to be metabolized in the intracellular volume (Q_3), presumably by NOS and/or AR, and that metabolism is denoted *k*. $(PS)_1$ represents l-arg transport from the vascular space (Q_1), or the extravascular space (Q_2), to the intracellular space (Q_3), presumably via CAT. Whereas $(PS)_2$ represents diffusion of l-arg from the vascular space to the extravascular space.

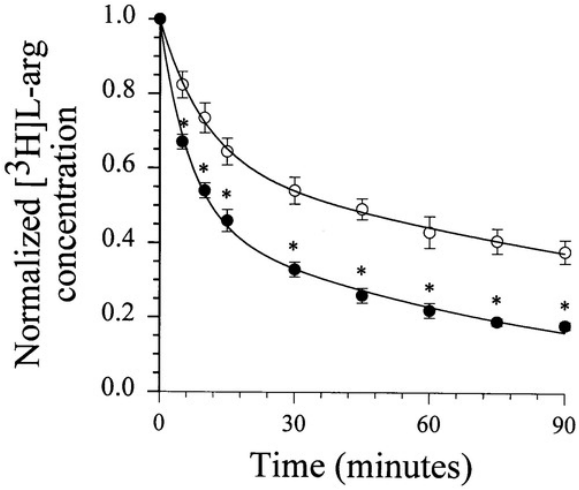

Fig. 2. The normalized concentration of [^{3}H]l-arginine in the perfusate of the lung during the 90-min perfusion period. The *open circles* are from control lungs and the *closed circles* are from silica-exposed lungs. The normalized concentration of [^{3}H]l-arg was significantly lower $(P < 0.05)$ at all time points studied, demonstrating that [^{3}H]l-arg uptake was greater in the silica-exposed lungs.

For each condition, the data ($d_i\ (t_j\ ),\ i$ denoting the individual experiment and *j* the time sample) were used to estimate the unknown model parameters, $\theta\ = (Q_3,\ (PS)_1, k)$. Because of the potentially high correlations between parameters in such a compartmental model, optimal parameter triples were obtained using two different methods of weighting the data. First, each individual experiment's optimal parameters, $\hat{\theta}_i$, were obtained by minimizing the individual sum-of-square error, $SS(\theta_i\ ) = \sum_{j=1}^{8}(c_1(t_j;\theta_i\ ) - d_i\ (t_j\ ))^2$, between model and experimental data. Here, we have used the notation $c_1(t_j;\theta_i\ )$ to explicitly denote the dependence of c_1 upon the model parameters. Optimization was performed using Matlab fmincon optimization routine (The MathWorks, Natick, MA), together with model equations solved using Matlab's ode23tb (a low order, stiff differential equations solver). Second, the entire data set for each condition was fit to a single set of parameters. That is, for each condition, a single (Q_3, $(PS)_1$,k) was found for the condition's full data set; obtained by minimizing the total sum-of-square error, $SS(\theta)\ =$ $\sum_{i=1}^{n}\ \ \sum_{j=1}^{8}(c_1(t_j;\theta\ ) - d_i\ (t_j\ ))^2$ (here, n denotes the number of experiments within a condition). In the latter optimization, 95% nonlinear confidence regions about the optimum, $\hat{\theta}$, in the three-dimensional parameter space were calculated[23] as shown in Figure 3. For the sum of squares surface, we used $F(3{,}37;\ 0.05)\ =\ 2.86$ and $F(3{,}61;\ 0.05)\ =\ 2.76$, for control and silica exposure, respectively.

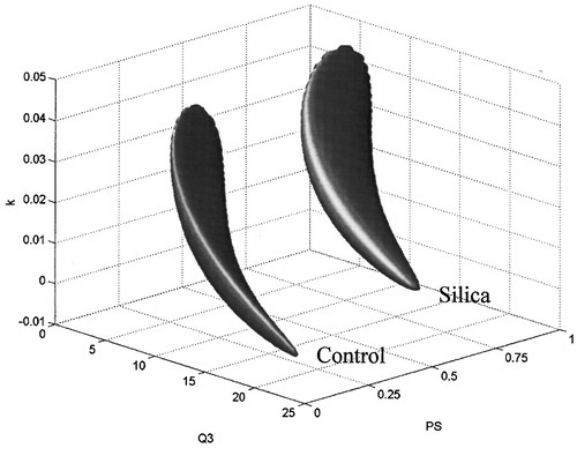

Fig. 3. The 95% nonlinear confidence regions for (Q_3, $(PS)_1$,*k*) after fitting all the data, within an experimental condition, simultaneously to a single set of parameters. Each surface represents the region

$$\mathrm{SS}(\theta) \le \mathrm{SS}(\hat{\theta})\left[1 + \frac{P}{N-P}\right] F(P, N-P;\ \alpha),$$

where $P\ =\ 3$, $N\ =\ 8n$ ($n\ =\ 5$ for control, $n\ =\ 8$ for silica exposed), and $\alpha\ =\ 0.05$.

Determination of mRNA and Protein

To determine if *in vivo* silica exposure had an affect on NOS protein expression, and NOS and CAT mRNA expression, Western blots and RT-PCR were done as described above. Three days after exposure the lungs from six control rats and four rats instilled with silica were harvested, immediately frozen in liquid nitrogen, and stored at −70°C. At a later time, the lung tissue was prepared as above and assayed for eNOS and iNOS protein, as well as for eNOS, iNOS, CAT-1, and CAT-2 mRNA as described above.

Statistics

Data are shown as mean ± SE. The control lungs were compared with the silica lungs using a one-way analysis of variance (ANOVA), and significant differences were identified using a Neuman-Keuls *post-hoc* test[24]. Differences were considered significant when $P < 0.05$.

Results

The silica exposure resulted in increases in measured variables consistent with lung injury 3–14 d after exposure (Table 1). At a constant perfusate flow rate, the isolated lungs from silica-exposed rats had a higher Pa. At a constant tidal volume, the isolated lungs from silica-exposed rats had a lower Cdyn. After perfusion, the lungs from silica-exposed lungs had higher wet and dry weights with little difference in the wet-to-dry weight ratios.

Table 1. Silica exposure causes lung injury

	Control	**Silica**
Pa (mm Hg)	6.2 ± 0.5	8.8 ± 0.5*
Cdyn (ml/mm Hg)	1.31 ± 0.26	0.37 ± 0.05*
Wet weight (*g*)	1.64 ± 0.27	5.05 ± 0.43*
Dry weight (*g*)	0.25 ± 0.02	0.81 ± 0.04*

Mean ± SE.

* Different from control, $P < 0.01$.

The [^{3}H]l-glucose uptake was significantly greater in silica-treated lungs compared with controls, 3–14 d after exposure (Figure 4A). The l-glucose equilibrated with an extracellular tissue volume (Q_2) of 0.57 ± 0.11 ml in the control lungs and 2.62 ± 0.27 ml in the silica lungs (different from control, $P < 0.005$). This indicates that a significant fraction of the greater wet weights in the silica lungs was extracellular water accessible via the perfusate (Table 1). The permeability-surface area product (PS_{glc}) for l-glc was also greater ($P < 0.05$) in the silica-treated than in the control lungs (0.24 ± 0.04 ml/min and 0.09 ± 0.05 ml/min, respectively). Silica exposure was associated with an increase in [^{3}H]l-arg uptake 3–14 d after exposure, as shown in Figure 1. The total uptake by the end of the 90-min perfusion period was 62 ± 3% in the control lungs and 82 ± 1% in silica-exposed lungs ($P < 0.001$). When saturating concentrations of unlabeled l-arg were included in the perfusate (Figure 4B), the [^{3}H]l-arg uptake results were not significantly different from the [^{3}H]l-glc results.

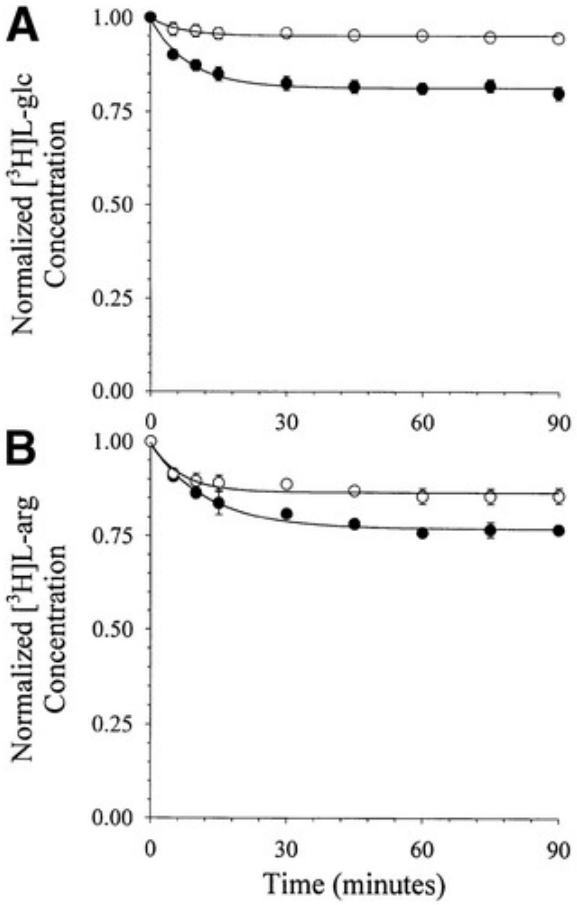

Fig. 4. (*A*) The normalized concentration of [^{3}H]l-glucose in the perfusate of the lung during the 90-min perfusion period. The *open circles* are from control lungs and the *closed circles* are from silica-exposed lungs. The normalized concentration of [^{3}H]l-glc was significantly lower ($P < 0.05$) at all time points studied, demonstrating that [^{3}H]l-glc uptake was greater in the silica exposed lungs. (*B*) The normalized concentration of [^{3}H]l-arg from the perfusate of the lung during 90-min perfusion with a saturating concentration of unlabeled l-arg as described in Materials and Methods. The *open circles* are from control lungs and the *closed circles* are from silica-exposed lungs. The normalized concentration of [^{3}H]l-arg was significantly lower ($P < 0.05$) from 30 min to 90 min, demonstrating that nonspecific [^{3}H]l-arg uptake was greater in the silica-exposed lungs.

Table 2 summarizes the parameters obtained when the model was fit to each individual data set from the tracer l-arg experiments. Both kQ_3 and $(PS)_1$ were significantly greater in the silica treated lungs, suggesting that both l-arg metabolism and l-arg uptake were increased by silica treatment. The individual fit results of Table 2 compare favorably with those obtained by fitting all the data, within an experimental condition, simultaneously to the model using a single set of parameters: $kQ_3 = 0.11$ ml/min and $(PS)_1 = 0.22$ ml/min for controls; $kQ_3 = 0.29$ ml/min and $(PS)_1 = 0.61$ ml/min for silica exposed lungs. The 95% nonlinear confidence regions about the $\hat{\theta}$ for each condition (Figure 3) are widely separated, further demonstrating the significant impact of silica treatment on [^{3}H]l-arg uptake.

Table 2. Summary of parameters from individual model fits

	Control	**Silica**	***P* Value***
n	5	8	
Q_2 (*ml*)	0.57 ± 0.11	2.62 ± 0.27	0.0003

PS_{glc} (*ml/min*)	0.09 ± 0.05	0.24 ± 0.04	0.046
kQ_3 (*ml/min*)	0.10 ± 0.01	0.38 ± 0.03	0.001
$(PS)_1$ (*ml/min*)	0.28 ± 0.05	0.63 ± 0.07	0.0003

Mean ± SE.

* Compared with control.

The greater [^{3}H]l-arginine uptake was associated with increased l-arg metabolism. On TLC the fractions at both 0.31 and 0.66 were observed to increase as perfusion time increased. There was no detectable fraction at 1.00, indicating that l-argininosuccinate was not a significant product of l-arg metabolism in these perfused lungs. Figure 5 demonstrates that the portion of ^{3}H in the perfusate appearing as l-orn and l-cit was significantly increased by silica treatment compared with controls. Figure 6 demonstrates that there was significantly more NO_X and urea accumulation in the perfusate of the silica-exposed lungs compared with controls at the end of 90 min.

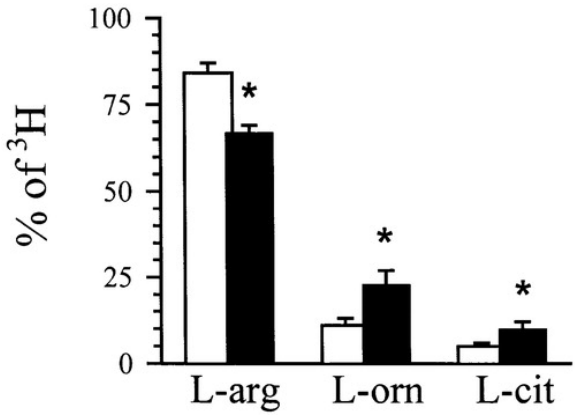

Fig. 5. The % of ^{3}H in the perfusate at 90 min as l-arg, l-orn, and l-cit; the *open bars* are control lungs and the *solid bars* are silica-exposed lungs. There was significantly less ^{3}H as l-arg and significantly more ^{3}H as l-orn and l-cit in the silica-exposed lungs.

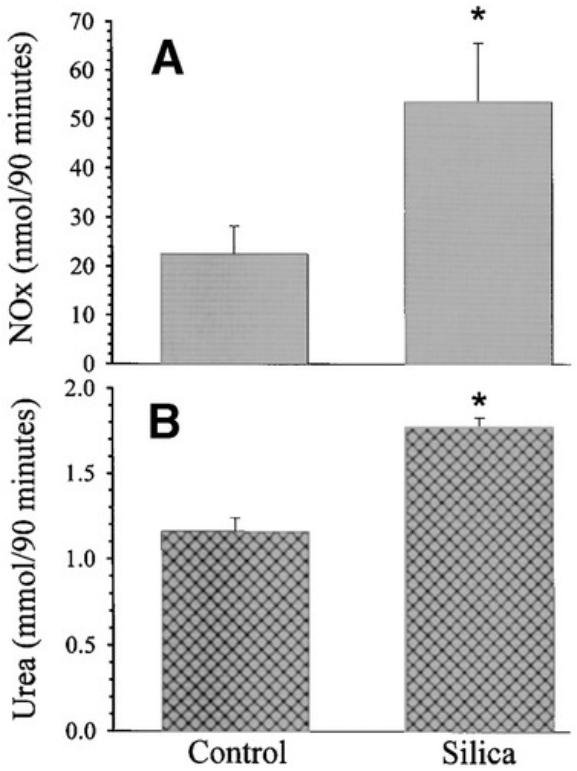

Fig. 6. The accumulation of NO_x (*A*) and urea (*B*) in the perfusate at 90 min in the control and silica-exposed lungs. The accumulation of both NO_x and urea were significantly increased in silica-exposed lungs. Note that the accumulation of urea is ~ 2 orders of magnitude greater than the accumulation of NO_x.

Western blot analysis of lungs revealed somewhat lighter bands for eNOS in silica-exposed compared with control lungs 3 d after exposure (Figure 7); however, the change in lung cellular composition makes this difficult to interpret. eNOS mRNA was not detectable by RT-PCR in either control or silica-exposed lungs 3 d after exposure. On the other hand, iNOS protein (Western blot analysis), which was not detectable in control lungs, was clearly present in silica-exposed lungs after 3 d (Figure 8), and the results were similar for iNOS mRNA (RT-PCR) (Figure 9). The silica-exposed lungs had nearly an 8-fold greater CAT-1 mRNA (Figure 10) and CAT-2 mRNA (Figure 11) compared with controls 3 d after exposure. Taken together, these results suggest that silica exposure resulted in both an induction of iNOS as well as CAT-1 and CAT-2.

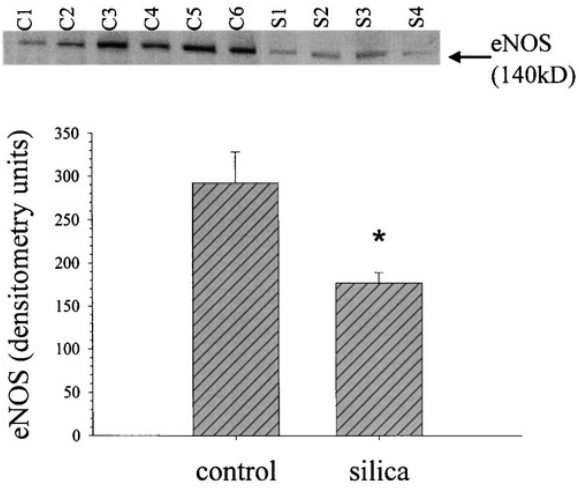

Fig. 7. The eNOS protein from lungs of control rats (C1–C6) and silica-exposed rats (S1–S4). The *bar graph* is the densitometric data from the Western blot, and reveals a lower level of eNOS protein in the silica-exposed rat lungs compared with control rat lungs.

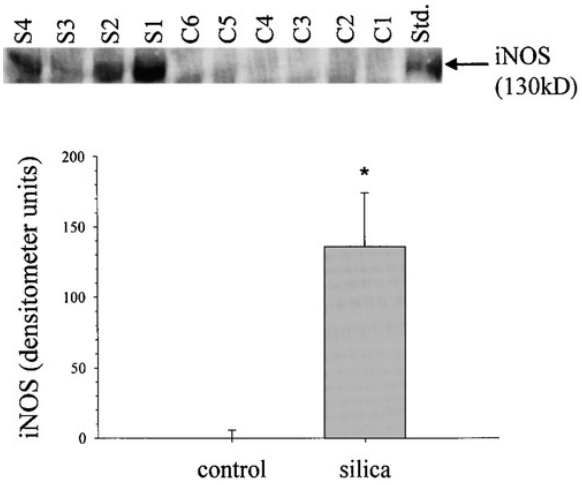

Fig. 8. The iNOS protein from lungs of control rats (C1–C6) and silica-exposed rats (S1–S4). The *bar graph* is the densitometric data from the Western blot. iNOS protein was not detectable in control rat lungs, but was detectable in the silica-exposed rat lungs.

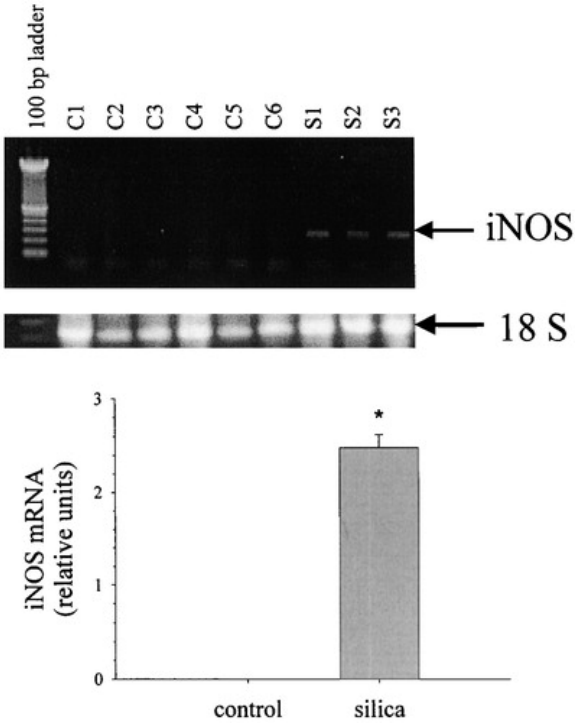

Fig. 9. The iNOS mRNA and 18S RNA from lungs of control rats (C1–C6) and silica-exposed rats (S1–S3). The *bar graph* is the densitometric data from the RT-PCR. iNOS mRNA was not detectable in control rat lungs, but was detectable in the silica-exposed rat lungs.

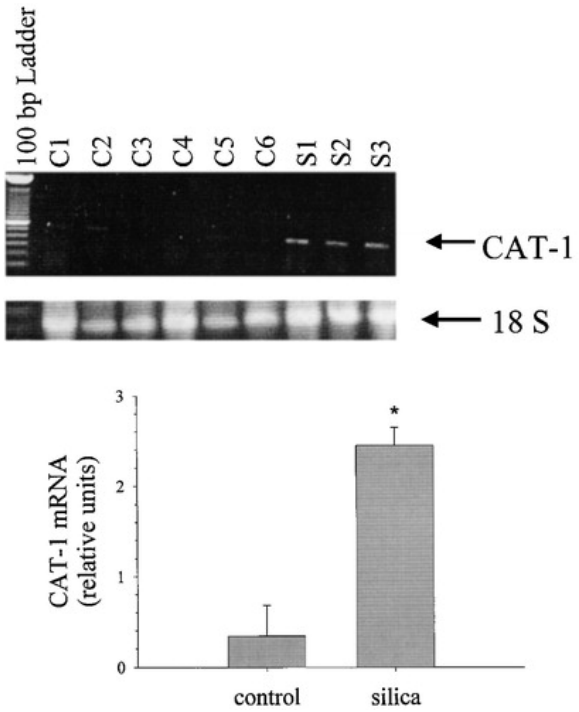

Fig. 10. The CAT-1 mRNA and 18S RNA from lungs of control (C1–C6) and silica-exposed (S1–S3) rats. The *bar graphs* are the densitometric data from the RT-PCR. CAT-1 mRNA was detectable in control rat lungs, and was ~ 8-fold greater in silica-exposed rat lungs compared with control rat lungs.

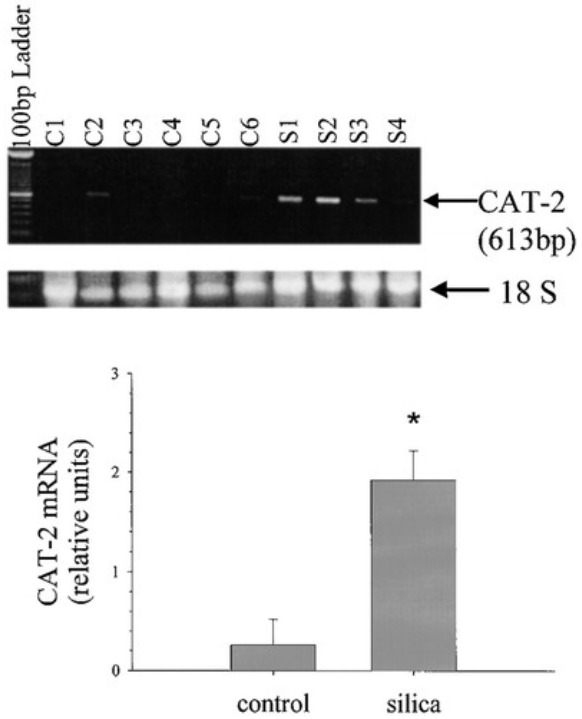

Fig. 11. The CAT-2 mRNA and 18S RNA from lungs of control (C1–C6) and silica-exposed (S1–S4) rats. The *bar graph* is the densitometric data from the RT-PCR. CAT-2 mRNA was detectable in control rat lungs, and was ~ 8-fold greater in silica-exposed rat lungs compared with control rat lungs.

Discussion

The main findings of this study were that in the intact lung (*i*) silica exposure increased l-arg metabolism via NOS and arginase, and (*ii*) the increased l-arg metabolism was associated with increased uptake of l-arg from the vascular space. The mRNA results suggest that the increase in l-arg uptake involved increased CAT-1 and CAT-2.

The decrease in eNOS protein is interesting and leads to the speculation that perhaps iNOS induction decreased eNOS expression. However, the increase in dry weight of the lung suggests a change in cellular composition of the lung. The Western blots were done on an aliquot of protein, and the cellular source of the protein would contain a much smaller proportion of endothelial cell–derived protein in the silica treated lungs compared with controls. Thus, the change in cellular composition of the lung could account for the decrease in eNOS protein expression seen in whole-lung homogenates. We were unable to detect eNOS mRNA in either control or silica-exposed lungs, suggesting that the steady-state levels of eNOS mRNA were below the levels detectable by our assay. Previously, using the same RT-PCR system, lungs from control rats had undetectable eNOS mRNA, whereas lungs from rats exposed to chronic hypoxia had detectable levels of eNOS mRNA[20].

The urea production was increased by silica exposure. It is of interest to note that arginase appears to be the major l-arg metabolic enzyme in the lung, because the accumulation of NO in the perfusate was only ~ 2% of the accumulation of urea in the perfusate. This is consistent with the study of Que and coworkers[9], wherein NOS activity was found to be ~ 1.5% of arginase activity in the rat lung. The silica-induced increase in urea production may be involved in polyamine synthesis via l-orn production, which is in turn involved in tissue inflammation and repair[17, 25, 26]. We did not establish if arginase was induced by silica exposure. Although arginase induction has been shown in other models of inflammatory lung damage[9, 26], further studies will be needed to determine if the silica-induced increase in urea production was due to induction of protein and/or increased enzymatic activity.

l-arginine is a substrate for both NOS and arginase. Thus, coinduction of NOS and arginase may result in competition between the two enzymes for available l-arg. For example, in murine macrophages[27] and rat alveolar macrophages[28] treated with LPS, inhibiting arginase activity increased NO production[27]. Furthermore, it has been found that metabolic products of NOS may inhibit NOS and/or arginase activity. For example, *N* $^{\omega}$-hydroxy-l-arginine, an intermediate in the oxidation of l-arg to l-cit and NO by NOS, has been found to be an inhibitor of arginase[29-31]. Similarly, it has been reported that nitrite inhibits NOS activity[32]. Thus, although both NOS and arginase are induced by silica exposure, the inter-relationship between NOS and arginase activity appears to be quite complex.

Kinetic studies of l-arg uptake have been performed in pulmonary arterial endothelial cells[11, 13, 32] or pulmonary arterial vascular smooth muscle[12]. A time course of 30–60 s was used, so that unidirectional uptake could be assumed. However, in an isolated lung preparation, it is impossible to measure the uptake of l-arg from the vascular space over this time course, because l-arg uptake is relatively slow compared with the lung transit time. Thus, we elected to study uptake over a longer time course, which required the development of the mathematical model to evaluate l-arg uptake kinetics. The mathematical model represented in Equations 4-6 for the calculation of PS products for l-arg and l-glc is based on the following assumptions. First, we assume linear uptake kinetics for [^{3}H]l-arg and [^{3}H]l-glc

(i.e., only the tracer l-arg concentration studies are modeled). Second, within the three compartments, Q_1, Q_2, and Q_3, concentrations are treated as uniform. Third, we assume that l-arg within the l-glc space (Q_2) has similar access to specific l-arg transporters as in the vascular space (Q_1). Finally, we assume that there is a nonspecific transport of l-arg into the l-glc space (Q_2). Within the limitations of these assumptions, we found that this model could describe the l-arg uptake kinetics in the whole lung, and the changes in uptake kinetic associated with silica-induced lung injury.

We found that the uptake of [^{3}H]l-arg was significantly increased by silica exposure. The model explanation for the increase in l-arg uptake included an increase in both extravascular volume (Q_2) and $\mathrm{PS}_{\mathrm{glc}}$ with silica exposure. The increase in Q_2 with silica exposure was roughly in proportion to the increase in wet weight. Within the assumption that the l-glc data reflects the nonspecific uptake of l-arg by the lung, an interpretation of these findings is that part of the silica exposure increase was due to increased nonspecific uptake of l-arg and dilution in a larger extracellular tissue volume. However, in addition, there was an increase in the specific uptake of l-arg (i.e., in that portion of the l-arg transport that was inhibited by the saturating l-arg concentrations). This result does not distinguish between an increase in transporter density or an increase in the cell surface area accessible to the [^{3}H]l-arg delivered via the perfusate. Assuming that cell surface area is proportional to tissue volume, the results suggest that an increase in the cell surface area accessible to the [^{3}H]l-arg delivered via the perfusate contributed to the increase in [^{3}H]l-arg uptake. However, the greater CAT-1 and CAT-2 mRNA seen with silica exposure are consistent with an increase in transporter density. Thus, it would appear that both an increase in the transporter density on the cell, as well as an increase in the cell surface area accessible to the l-arg delivered in the perfusate, may contribute to the greater specific l-arg uptake we found in the silica-exposed lungs.

The cell type involved in the increase in l-arg transport found in the silica-treated lungs was not directly determined. Again, the model only requires two tissue compartments to fit the data. Thus, all cell types involved in specific l-arg uptake and metabolism are lumped. This is probably an oversimplification, but again, there are no systematic deviations from the model fit of the data that would suggest that additional model parameters would be separable without additional experiments designed to target specific processes or cell types. On the other hand, macrophages and neutrophils contribute substantially to the increase in lung tissue mass seen with silica exposure[1, 4, 8]. We have previously found that l-arg uptake is increased in alveolar macrophages and neutrophils harvested from silica-exposed rat lungs[8]. Taken together, these findings would suggest that macrophages and neutrophils contributed to the increase in l-arg transport and metabolism. A contribution of pulmonary arterial endothelial cells, which would be the cell type in direct contact with the perfusate, is consistent with studies in cells in culture wherein treatment with inflammatory mediators increased the l-arg transporter maxima[11-13, 33].

The mathematical model results are also consistent with an increase in l-arg metabolism caused by silica treatment. This is reflected in the 2.8-fold increase in the parameter kQ_3 in the silica-exposed lungs**.** The parameter kQ_3 represents the product of the intracellular volume (Q_3) and metabolism of l-arg (k). The metabolism of l-arg includes contributions from both NOS and AR. However, other enzymatic pathways, such as arginine decarboxylase, or nonenzymatic pathways, such as protein synthesis, may also contribute to l-arg metabolism in the lung. In our mathematical model, there is not

enough data to determine the relative contributions of all of the various metabolic pathways that can affect intracellular l-arg concentration. Furthermore, the affect of changes in l-arg metabolism on the intracellular l-arg concentration is complicated by the presence of enzymes that recycle l-orn and/or l-cit to l-arg. In endothelial cells it has been demonstrated that argininosuccinate synthetase, one of these recycling enzymes, is upregulated by cytokine treatment[34]. However, despite these limitations, interpreting the increase in kQ_3 as an increase in l-arg metabolism by NOS and AR is consistent with the increase in perfusate accumulation of NO_x and urea in the silica-treated lungs. However, the respective tracer concentration data alone are not sufficient to differentiate between the contributions of NOS versus AR to kQ_3.

In conclusion, we found that silica exposure increased iNOS and l-arg metabolism to both NO and urea in the intact lung. We found that arginase was the primary l-arg– metabolizing enzyme in the normal lung. Finally, we found that l-arg uptake and CAT-1 and CAT-2 mRNA were increased by silica exposure. These results may have important implications in the development of therapeutic strategies aimed at manipulating NO production in lung inflammation.

The authors wish to thank Carol J. Thomas, James Morrisey, and Linda Rehorst-Paea for technical assistance. This work was supported in part by a grant from the March of Dimes Birth Defects Foundation, and by National Heart, Lung and Blood Institute Grant HL-04050 (L.G.C.).

References

1. DiMatteo M., Antonini J. M., Van Dyke K., Reasor M. J. Characteristics of the acute-phase pulmonary response to silica in rats. J. Toxicol. Environ. Health47199693108
2. Graham W. G. B. Silicosis. Clin Chest Med131992253267
3. Blackford J. A., Antonini J. M., Castranova V., Dey R. D. Intratracheal instillation of silica up-regulates inducible nitric oxide synthase gene expression and increases nitric oxide production in alveolar macrophages and neutrophils. Am. J. Respir. Cell Mol. Biol.111994426431
4. Quinlan T. R., Berube K. A., Hacker M. P., Taatjes D. J., Timblin C. R., Goldberg J., Kimberley P., O'Shaughnessey P., Hemenway D., Torino J., Jimenez L. A., Mossman B. T. Mechanisms of asbestos-induced nitric oxide production by rat alveolar macrophages in inhalation and in vitro models. Free Radic. Biol. Med.241998778788
5. Janne J, Alhonen L., Leinonen P. Polyamines: from molecular biology to clinical applications. Ann. Med.231991241259
6. Li H., Meininger C. J., Hawker J. R., Haynes T. E., Kepka-Lenhart D., Mistry S. K., Morris S. M., Wu G. Regulatory role of arginase I and II in nitric oxide, polyamine and proline syntheses in endothelial cells. Am. J. Physiol. Endocrinol. Metab.2802001E75E82
7. Nelin L. D., Nash H. E., Chicoine L. G. Cytokine treatment increases arginine metabolism and uptake in bovine pulmonary arterial endothelial cells. Am. J. Physiol. Lung Cell. Mol. Physiol.2812001L1232L1239
8. Schapira R. M., Wiessner J. H., Morrisey J. F., Almagro U. A., Nelin L. D.l-arginine uptake and metabolism by lung macrophages and neutrophils following intratracheal instillation of silica in vivo. Am. J. Respir. Cell Mol. Biol.191998308315
9. Que, L. G., S. P. Kantrow, C. P. Jenkinson, C. A. Piantadosi, and Y. C. Huang. 1998. Induction of arginase isoforms in the lung during hyperoxia. Am. J. Physiol. 275(Lung Cell Mol. Physiol. 19):L96–L102.
10. Setoguchi K., Takeya M., Akaike T., Suga M., Hattori R., Maeda H., Ando M., Takahashi K.Expression of inducible nitric oxide synthase and its involvement in pulmonary granulomatous inflammation in rats. Am. J. Pathol.149199620052022

11. Lind D. S., Copeland E. M., Souba W. W.Endotoxin stimulates arginine transport in pulmonary artery endothelial cells.Surgery1141993199205
12. Durante, W., L. Liao, and A. I. Schafer. 1995. Differential regulation of l-arginine transport and inducible NOS in cultured vascular smooth muscle cells. Am. J. Physiol. 268(Heart Circ. Physiol. 37):H1158–H1164.
13. Greene, B., A. J. Pacitti, and W. W. Souba. 1993. Characterization of l-arginine transport by pulmonary artery endothelial cells. Am. J. Physiol. 264(Lung Cell Mol. Physiol. 8):L351–L356.
14. Hattori, Y., K. Kasai, and S. S. Gross. 1999. Cationic amino acid transporter gene expression in cultured vascular smooth muscle cells and in rats. Am. J. Physiol. 276(Heart Circ. Physiol. 45):H2020–H2028.
15. Schapira R. M., Ghio A. J., Effros R. M., Morrisey J., Dawson C. A., Hacker A. D.Hydroxyl radicals are formed in the rat lung after asbestos instillation in vivo. Am. J. Respir. Cell Mol. Biol.101994573579
16. Schapira R. M., Ghio A. J., Effros R. M., Morrisey J., Almagro U. A., Dawson C. A., Hacker A. D. Hydroxyl radical production and lung injury in the rat lung following silica or titanium dioxide instillation in vivo. Am. J. Respir. Cell Mol. Biol.121995220226
17. Cook, H. T., A. Jansen, S. Lewis, P. Largen, M. O'Donnell, D. Reaveley, and V. Cattell. 1994. Arginine metabolism in experimental glomerulinephritis: interaction between nitric oxide synthase and arginase. Am. J. Physiol. 267(Renal Fluid Electrolyte Physiol. 36):F646–F653.
18. Fike, C. D., M. R. Kaplowitz, C. J. Thomas, and L. D. Nelin. 1998. Chronic hypoxia decreases nitric oxide production and endothelial nitric oxide synthase in newborn pig lungs. Am. J. Physiol. 274(Lung Cell Mol. Physiol. 18):L517–L526.
19. Chomczynski P., Sacchi N. Single-step method of RNA isolation by acid guanidinium thiocynate-phenol-chloroform extraction. Anal. Biochem.1621987156159
20. Resta, T. C., L. G. Chicoine, J. L. Omdahl, and B. R. Walker. 1999. Maintained upregulation of pulmonary eNOS gene and protein expression during recovery from chronic hypoxia. Am. J. Physiol. 276(Heart Circ. Physiol. 45):H699–H708.
21. Resta, T. C., T. L. O'Donaughy, S. Earley, L. G. Chicoine, and B. R. Walker. 1999. Unaltered vasoconstrictor responsiveness after iNOS inhibition in lungs from chronically hypoxic rats. Am. J. Physiol. 276(Lung Cell Mol. Physiol. 20):L122–L130.
22. Bongard R. D., Roerig D. L., Johnston M. R., Linehan J. H., Dawson C. A. Influence of temperature and plasma protein on doxorubicin uptake by isolated lungs. Drug Metab. Dispos.211993428434
23. Bates, D. M., and D. G. Watts. 1988. Nonlinear Regression Analysis and its Applications. John Wiley & Sons, New York.
24. Sokal, R. F., and F. J. Rohlf. 1980. Biometry. W. H. Freeman and Company, New York.
25. Schearer, J. D., J. R. Richards, J. D. Mills, and M. D. Caldwell. 1997. Differential regulation of macrophage arginine metabolism: a proposed role in wound healing. Am. J. Physiol. 272(Endocrinol. Metab. 35):E181–E190.
26. Sonoki T., Nagasaki A., Gotoh T., Takiguchi M., Takeya M., Matsuzaki H., Mori M. Coinduction of nitric oxide synthase and arginase I in cultured rat peritoneal macrophages and rat tissues in vivo by lipopolysacchride. J. Biol. Chem.272199736893693
27. Chang, C. I., J. C. Liao, and L. Kuo. 1998. Arginase modulates nitric oxide production in activated macrophages. Am. J. Physiol. 274(Heart Circ. Physiol. 43):H342–H348.
28. Hey C., Boucher J. L., Vadon-Le Goff S., Ketterer G., Wessler I., Racke K. Inhibition of arginase in rat and rabbit alveolar macrophages by Nω-hydroxy-D,l-indospincine: effects on l-arginine utilization by nitric oxide synthase. Br. J. Pharmacol.1211997395400
29. Buga, G. M., R. Singh, S. Pervin, N. E. Rogers, D. A. Schmitz, C. P. Jenkinson, S. D. Cederbaum, and L. J. Ignarro. 1996. Arginase activity in endothelial cells: inhibition by NG-hydroxy-l-arginine during high output NO production. Am. J. Physiol. 271(Heart Circ. Physiol. 40):H1988–H1998.

30. Hecker M., Nematollahi H., Hey C., Busse R., Racke K. Inhibition of arginase by NG-hydroxy-l-arginine in alveolar macrophages: implications for the utilization of l-arginine for nitric oxide synthesis. FEBS Lett.3591995251254
31. Waddington, S. N., F. W. K. Tam, H. T. Cook, and V. Cattell. 1998. Arginase activity is modulated by IL-4 and HOArg in nephritic glomeruli and mesangial cells. Am. J. Physiol. 274 (Renal Physiol. 43):F473–F480.
32. Hrabek A., Bajor T., Temesi A., Meszaros G. The inhibitory effect of nitrite, a stable product of nitric oxide (NO) formation, on arginase. FEBS Lett.3901996203206
33. Pan M., Wasa M., Ryan U., Souba W. Lipopolysaccharide and tumor necrosis factor stimulate lung microvascular arginine uptake, a response attenuated by dexamethasone. JPEN2019965055
34. Simmons W. W., Ungureanu-Longrois D., Smith G. K., Smith T. W., Kelly R. A.Glucocorticoids regulate inducible nitric oxide synthase by inhibiting tetrahydrobiopterin synthesis and l-arginine transport. J. Biol. Chem.27119962392823937

Abbreviations

arginase, AR; inducible nitric oxide synthase, iNOS; l-arginine, l-arg; nitric oxide, NO; nitrite/nitrate, NOX; thin-layer chromatography, TLC.